
Responses to herbicides of Arctic and temperate microalgae grown under different light intensities

Du Juan ¹, Izquierdo Disney ², Xu Hai-Feng ³, Beisner Beatrix ⁴, Lavaud Johann ^{5, 6}, Ohlund Leanne ⁷, Sleno Lekha ⁷, Juneau Philippe ^{2, *}

¹ Department of Biological Sciences, Université du Québec à Montréal-GRIL-TOXEN, Succ Centre-Ville, Montréal, Canada

² Department of Biological Sciences, Université du Québec à Montréal-GRIL-EcotoQ-TOXEN, Succ Centre-Ville, Montréal, Canada

³ School of Life Sciences, and Hubei Key Laboratory of Genetic Regulation and Integrative Biology, Central China Normal University, Wuhan, 430079, Hubei, China

⁴ Department of Biological Sciences, Groupe de Recherche Interuniversitaire en Limnologie (GRIL), Université du Québec à Montréal, Canada

⁵ TAKUVIK International Research Laboratory IRL3376, Université Laval (Canada) - CNRS (France), Pavillon Alexandre-Vachon, 1045 Av. de la Médecine, Local 2064, G1V 0A6, Québec, Canada

⁶ LEMAR-Laboratory of Environmental Marine Sciences, UMR6539, CNRS/Univ Brest/Ifremer/IRD, Institut Universitaire Européen de La Mer, Technopôle Brest-Iroise, Rue Dumont d'Urville, 29280, Plouzané, France

⁷ Chemistry Department, Université du Québec à Montréal-EcotoQ-TOXEN, Succ Centre-Ville, Montreal, Quebec, H3C 3P8, Canada

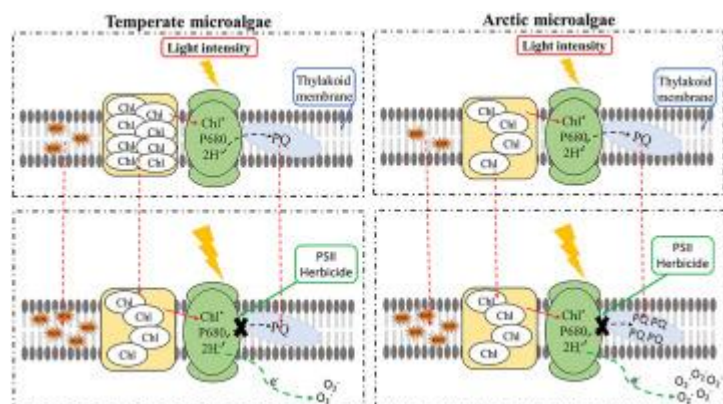
* Corresponding author : Philippe Juneau, email address : juneau.philippe@uqam.ca

Abstract :

In aquatic ecosystems, microalgae are exposed to light fluctuations at different frequencies due to daily and seasonal changes. Although concentrations of herbicides are lower in Arctic than in temperate regions, atrazine and simazine, are increasingly found in northern aquatic systems because of long-distance aerial dispersal of widespread applications in the south and antifouling biocides used on ships. The toxic effects of atrazine on temperate microalgae are well documented, but very little is known about their effects on Arctic marine microalgae in relation to their temperate counterparts after light adaptation to variable light intensities. We therefore investigated the impacts of atrazine and simazine on photosynthetic activity, PSII energy fluxes, pigment content, photoprotective ability (NPQ), and reactive oxygen species (ROS) content under three light intensities. The goal was to better understand differences in physiological responses to light fluctuations between Arctic and temperate microalgae and to determine how these different characteristics affect their responses to herbicides. The Arctic diatom *Chaetoceros* showed stronger light adaptation capacity than the Arctic green algae *Micromonas*. Atrazine and simazine inhibited the growth and photosynthetic electron transport, affected the pigment content, and disturbed the energy balance between light absorption and utilization. As a result, during high light adaptation and in the presence of herbicides, photoprotective pigments were synthesized and NPQ was highly activated. Nevertheless, these protective responses were insufficient to prevent oxidative damage caused by herbicides in both species from both regions, but at different extent depending on the species. Our study

demonstrates that light is important in regulating herbicide toxicity in both Arctic and temperate microalgal strains. Moreover, eco-physiological differences in light responses are likely to support changes in the algal community, especially as the Arctic ocean becomes more polluted and bright with continued human impacts.

Graphical abstract



Highlights

- Photoadaptation processes are different between Arctic and temperate microalgae.
- Arctic and temperate microalgae have different sensitivities to two herbicides.
- High light enhances the impacts of herbicides on energy dissipation and photosynthesis of microalgae.
- Atrazine removal by algae increased under high light.
- These findings have applications for Arctic and temperate microalgae living in fluctuating light environments.

Keywords : Marine microalgae, Atrazine, Simazine, Light, Photoadaptation, Ecotoxicology.

79 **Introduction**

80 Light intensity is one of the most important environmental factors influencing the
81 growth of photosynthetic organisms (Edwards et al. 2015). In aquatic environments,
82 microalgae experience intense light fluctuations due to the daily sunlight exposure and
83 seasonal variation (Wagner et al. 2006). Meanwhile, turbidity in the water and
84 refraction of sunlight cause light intensity changes at different depths, with photon flux
85 scarcer in the deeper layers of the water column than at the surface (Dubinsky and
86 Stambler 2009). To cope with the fluctuating light environments, photosynthetic
87 organisms have evolved diverse phenotypic adjustments including photoadaptation
88 processes (Deblois et al. 2013a, Handler 2017). Photoadaptation to low or high light

89 environments involves changes at the gene level leading to modification of their
90 physiology, biochemistry, and morphology (Bellacicco et al. 2016, Deblois et al. 2013b).
91 Physiological photoprotection mechanisms of photosynthetic organisms include the
92 PSII repair cycle, changes in pigment, de novo synthesis of proteins, state transitions,
93 changes in energy efficiency transferred from the light-harvesting complex to reaction
94 centers (RCs), and non-photochemical quenching (NPQ) induced by activation of the
95 xanthophyll cycle (XC) (Deblois et al. 2013a, Dong et al. 2016, Hopes and Mock 2015).
96 Among them, NPQ is the fastest and most flexible response to light variation (Goss and
97 Lepetit 2015). In diatoms, the XC (de-epoxidation of diadinoxanthin to diatoxanthin)
98 is activated by the light-driven acidification of the thylakoid lumen resulting in the
99 accumulation of diatoxanthin. This process is a prerequisite for the formation of energy-
100 dependent quenching (qE) that is the major component of NPQ in diatoms (Lepetit et
101 al. 2017), which is not necessarily the case in plants and green algae (Allorent et al.
102 2013, Goss and Lepetit 2015).

103 As primary producers, microalgae constitute the basis of aquatic ecological trophic
104 networks. The diatom *Chaetoceros sp.* and the small flagellate prasinophyte
105 *Micromonas sp.* are dominant species in both Arctic and temperate regions (Balzano et
106 al. 2012, Balzano et al. 2017, Seoane et al. 2019). They are thus among the non-target
107 aquatic organisms exposed to pesticides (Chen et al. 2016). The effect of pesticides has
108 been predominantly studied in freshwater ecosystems compared to marine and estuarine
109 ecosystems (Dar et al. 2021, Dupraz et al. 2016). Herbicides are the most widely used
110 among the major pesticide classes, and their toxic effects mainly affect the growth,
111 photosynthesis, morphology, biochemical composition, and lipid content of microalgae
112 (DeLorenzo 2001, Sun et al. 2020). The deleterious effects of specific photosystem II
113 (PSII) inhibitor herbicides, such as atrazine and simazine, are primarily to reduce
114 photosynthetic efficiency by inhibiting photosynthetic electron transfer. It induces the
115 production of reactive oxygen species (ROS) and further damage the D1 protein of PSII
116 and biomolecules like pigments (Chalifour and Juneau 2011, Zhao et al. 2018). Some
117 studies have shown that short-term light changes can affect the toxicity of pesticides

118 (Baxter et al. 2016, Dong et al. 2016). However, very little is known about how
119 photoadaptation to different light intensities influences the response of marine
120 microalgae to herbicides.

121 Most of our knowledge regarding microalgal photoadaptation strategies and
122 pesticide effects is from temperate species (Gomes and Juneau 2017, Young and
123 Schmidt 2020). Microalgae have a rich evolutionary history due to their widespread
124 presence in various habitats, especially marine ecosystems, leading to a wide range of
125 adaptations, allowing them to thrive in a variety of environmental conditions (Lacour
126 et al. 2020). Polar microalgae adapted to permanently low temperatures and extreme
127 variation in irradiance due to seasonally changing ice-cover and day lengths (Handler
128 2017). Sea-ice of Arctic Ocean is gradually melting because of global warming,
129 increasing light availability at the sea surface (Osborne et al. 2018). Therefore, studying
130 the differences in the adaptation processes intrinsic to Arctic and temperate microalgae
131 can provide insights into how microalgae will cope with the changing aquatic
132 environment, including light intensity and herbicide presence. It is known that ice
133 melting may potentially cause an increase in pesticide concentrations in the Arctic
134 waters (Pućko et al. 2017), although at concentrations that will remain lower than the
135 ones found in temperate regions. Indeed, the main source of pesticides in Arctic is from
136 the long-range aerial transport and not the nearby agricultural activities as it is for
137 temperate regions (Schmale et al. 2018, Vorkamp and Riget 2014). In this study, we
138 aimed to determine the response to herbicides of Arctic and temperate microalgae
139 photoadapted to various light intensities and how various photoadaptation strategies
140 affect herbicide toxicity. Our comparison of eco-physiological responses of Arctic to
141 their temperate counterparts will facilitate the development of population growth
142 models for microalgae more generally, as models predicting microalgal biomass
143 changes due to light and contaminants generally use observations from only temperate
144 algae.

145

146 2. Materials and methods

147 2.1 Algal species and growth conditions

148 Temperate *Chaetoceros neogracile* (T-CN-CCMP1425), temperate *Micromonas*
149 *bravo* (T-MB-CCMP1646), and Arctic strain of *Micromonas polaris* (A-MP-
150 CCMP2099) were purchased from NCMA (National Contract Management
151 Association). The Arctic strain of *Chaetoceros neogracilis* (A-CN-RCC2279) was
152 obtained from the Roscoff culture collection (France). All species were cultivated in L1
153 marine medium (Guillard and Hargraves 1993) with a total volume of 100 mL medium
154 in 250 mL Erlenmeyer flasks. Microalgae were grown at three different light intensities
155 under white fluorescent tubes (Philips F72T8/TL841/HO, New York, NY, USA) (low
156 light intensity-40 $\mu\text{mol photons m}^{-2} \text{s}^{-1}$ (LL), medium light intensity-100 $\mu\text{mol photons}$
157 $\text{m}^{-2} \text{s}^{-1}$ (ML), and high light intensity-400 $\mu\text{mol photons m}^{-2} \text{s}^{-1}$ (HL)), intensities found
158 at the surface of the Arctic Ocean and in temperate area (Lepetit et al. 2017, Leu et al.
159 2010), at 14:10 h (light: dark) illumination cycle and shaken moderately twice a day.
160 Growth temperatures were 18 °C and 4 °C, respectively, for temperate and Arctic
161 species. Cells were periodically transferred to fresh growth media to keep them in their
162 exponential growth phase. The cells were cultured for more than ten generations in
163 these growth conditions. The cell numbers were counted using Multisizer 3 Coulter
164 Counter (Beckman Coulter Inc., USA). The calculation of growth rate (μ) is based on
165 the following formula: $\mu = (\ln N_n) - (\ln N_0) / (t_n - t_0)$, where μ = average specific growth
166 rate, N_0 , N_n indicate cell density (cells mL^{-1}) at respectively t_0 (beginning of the
167 experiment) and t_n (time, in days, after the beginning of the experiment).

168 2.2 Herbicide preparation and treatment

169 Atrazine and simazine used in this study came from Sigma-Aldrich (PESTANAL®,
170 analytical standard, Canada). Herbicide stock solutions were made in pure acetone (\geq
171 99%) and acetone concentration was 0.01% in the treatments, which was verified not
172 to be toxic to these microalgae. Six concentrations of atrazine and simazine were used
173 for the herbicide tests (0 $\mu\text{g L}^{-1}$, 5 $\mu\text{g L}^{-1}$, 25 $\mu\text{g L}^{-1}$, 50 $\mu\text{g L}^{-1}$, 100 $\mu\text{g L}^{-1}$, and 250 μg

174 L⁻¹). Cells were collected during their exponential growth phase and transferred to 1 L
175 Erlenmeyer flasks (with 350 mL growth medium) at a cell density of 2.5×10^5
176 (*Chaetoceros*) and 2.5×10^6 (*Micromonas*) cells mL⁻¹ respectively, and then exposed to
177 different concentrations of herbicides for 72 h under the three light conditions. Our
178 experimental design follows standard procedure for toxicological tests with algae, the
179 pH of the cultures did not change over the exposure period and all treatments were
180 performed in triplicate. Cell density and cell biovolume were evaluated at the end of
181 the experiment with a Multisizer 3 Coulter Counter particle analyzer (Beckman Coulter
182 Inc., USA).

183 2.3 Pigment content measurement

184 Algal cultures (25 mL) were collected after 72 h herbicide treatment through a
185 gentle filtration on 0.8µm filter membranes (Polytetrafluoroethylene; Xingya Purifyin
186 Company; China). Filters were immediately submerged in liquid nitrogen and placed
187 in 2 mL Eppendorf tubes, and then stored at -80 °C until analysis. Each sample was
188 added to 2 mL of 90% acetone to be extracted overnight at -20 °C before pigment
189 analysis. Cells in an ice container were broken for 20 s using an ultrasonic probe to
190 increase extraction efficiency. The samples were centrifuged (10000×g) at 4 °C for 10
191 min after the extraction. The supernatants were used to quantify the content of
192 chlorophyll (Chl *a*) and carotenoids (Car). A Cary 300 UV spectrophotometer (Varian,
193 USA) was used to determine the absorbance spectra (400–750nm) for each extracted
194 sample. Based on the equations from (Jeffrey and Humphrey 1975) and Seely et al.
195 (1972), the contents of Chl *a* and Car were calculated respectively.

196 2.4 Variable Chl *a* fluorescence measurement

197 The samples (3 mL) were measured at their growth temperature of 4 °C and 18 °C
198 after dark acclimation for 20 min. Fluorescence light curves performed with a
199 fluorometer of Water-PAM (Walz, Germany) were used to evaluate the maximum (Φ_M)
200 and operational (Φ'_M) PSII quantum yields, as well as the non-photochemical
201 quenching (NPQ) (Du et al. 2019). The light curve was obtained by using eight levels

202 of actinic light intensities (0, 46, 105, 188, 276, 427, 635, 906, and 1207 $\mu\text{mol photons}$
203 $\text{m}^{-2}\text{s}^{-1}$) with saturation pulses (3000 $\mu\text{mol photons m}^{-2} \text{s}^{-1}$, 800 ms). Φ_M , Φ'_M and NPQ
204 were computed according to the following equations: $\Phi_M = (F_M - F_0)/F_M$; $\Phi'_M = (F'_M -$
205 $F_S)/F'_M$ (Genty et al. 1989); $\text{NPQ} = (F_M - F'_M)/F'_M$ (Bilger and Björkman 1990).
206 Maximum relative electron transport rates ($r\text{ETR}_{\text{max}}$), maximum light efficiency usage
207 (α), and light saturation coefficient (E_k) were obtained by fitting the obtained values
208 according to (Eilers and Peeters 1988, Serodio and Lavaud 2011). To further assess the
209 PSII energy fluxes, the polyphasic increase in fluorescence transients was also captured
210 by a PEA fluorometer (Plant Efficiency Analyzer, UK). The OJIP transients were
211 generated by using a red light pulse of two seconds (3600 $\mu\text{mol photons m}^{-2} \text{s}^{-1}$) with a
212 maximum emission at 650 nm (Jiang et al. 2008). Table S1 provides a description of
213 each parameter.

214 2.5 Reactive oxygen species (ROS) measurement

215 Intracellular ROS content was determined by using a BD Accuri C6 flow
216 cytometer (Biosciences, San Jose, CA, USA). The fluorescent dye H_2DCFDA (2',7'-
217 dichlorodihydrofluorescein diacetate, Molecular probes, Eugene, OR, USA) was used.
218 More information about this method was described in (Stachowski-Haberkorn et al.
219 2013). Samples were analyzed after incubation in complete darkness for 30 min at room
220 temperature. To prevent possible signal variations due to herbicide influence on FL1
221 fluorescence, the mean FL1 values of H_2DCFDA -stained samples were divided by the
222 mean FL1 values of the same fresh samples analyzed for morphology. Results were
223 thus expressed as FL1 ratios.

224 2.6 Atrazine determination

225 The concentration of atrazine removed from the growth medium was calculated
226 by subtracting the concentration found in the sample (atrazine + growth medium +
227 microalgae) treated for 72 h from the abiotic control (atrazine + growth medium). To
228 measure atrazine concentration remaining in the growth medium i.e., removal capacity
229 of microalgae, cultures (in triplicate) were transferred to 250 mL flasks containing 100

230 mL of L1 growth media at cell concentrations indicated in section 2.2 for 72 h. Abiotic
231 controls, also in triplicate, were prepared using L1 medium without cells, and various
232 light intensities did not alter the atrazine concentration. After inoculation of the
233 microalgae in the medium, 2 mL aliquots of each flask were sampled and filtered on a
234 20 mm glass fiber filter (Type A/E, Pall Corporation, Michigan, USA) and stored in 1.5
235 mL Eppendorf tubes (polypropylene Safe-Lock tube, Canada). The filtrate was kept at
236 -80 °C until analysis. After 72 h, the same procedure was repeated with 2 mL of culture
237 for herbicide analysis. Before analysis, filtered media containing atrazine were thawed
238 and then filtered again through a 0.22 µm syringe filter (Millex-GV, Millipore, Billerica,
239 USA).

240 A stock solution of atrazine at 1 µg L⁻¹ was prepared in 50% methanol to perform
241 a calibration curve ranging from 0.5-20 µg L⁻¹. An internal standard (IS) working
242 solution of isotopically labeled atrazine-d₅ was prepared at 100 µg L⁻¹, 20 µL of which
243 was added to each sample or standard with 180 µL. Quantitative analysis of atrazine
244 was performed by QTRAP 5500 mass spectrometer (Sciex, Concord, ON, Canada) with
245 a Turbo-V electrospray ionization source in positive ion multiple reaction monitoring
246 (MRM) mode (Chalifour et al. 2016). Atrazine and IS were detected using MRM
247 transitions *m/z* 216-174 and 221-179 for quantitation (at collision-offset voltage 30 and
248 25 V). Ion source and MS parameters were as follows: ESI voltage, 5000 V; source
249 temperature, 500 °C; curtain gas, curtain gas, 35 psi; nebulizer and drying gases both
250 at 50 psi. Peak integration was performed using MultiQuant™ 3.0 (Sciex), using peak
251 area ratios of analyte/IS and linear regression of calibration curve for quantitation.

252 2.7 Statistical analyses

253 Statistical analyses were performed using Origin® 7.0 (Originlab Corporation,
254 Northampton, MA, USA). Two-way analysis of variance (ANOVA) was used to
255 determine the effect of treatments, and Tukey's honestly significant difference (Tukey's,
256 HSD) test was conducted to test the statistical significance of the differences between
257 means of various treatments. The assumption of normal distribution and homogeneity
258 of variances for all t-tests and ANOVAs presented were respectively tested using

259 Lilliefors' and Levene's tests. Two-way analysis of variance (ANOVA) to evaluate the
260 interactions between growth light conditions (LL, ML, and HL), and herbicide
261 concentrations. Contrast analysis was used when there were significant differences in
262 the studied variables between treatments. The EC₅₀ (half-maximum effective
263 concentration) values were calculated from the nonlinear least-square fits by using the
264 inverse of the regression curve (Juneau et al. 2001).

265

266 **3. Results**

267 **3.1 Effects of the growth light intensity on the ecophysiological characteristics of** 268 **the Arctic and temperate microalgae in absence of herbicides**

269 3.1.1 Growth rate, cell biovolume, pigment content, and ROS content

270 Growth rates of Arctic and temperate microalgae (except for T-MB) grown under
271 LL conditions were drastically lower than those under ML or HL conditions (Tukey's
272 HSD, $P < 0.05$, Table 1, Fig. 1-atrazine concentration = $0 \mu\text{g L}^{-1}$). Moreover, the growth
273 rates of Arctic microalgae (*C. neogracilis*-A-CN and *M. polaris*-A-MP) were lower
274 than their temperate counterparts (*C. neogracile*-T-CN, *M. bravo*-T-MB) under the
275 three different light intensities; the exception being for A-CN under LL condition. In
276 addition, the increasing trend of growth rate for Arctic microalgae was lower than that
277 of temperate counterparts when the light intensity was enhanced. Similarly, the cell
278 biovolume of two Arctic microalgae was smaller under LL condition compared to ML
279 and HL (Tukey's HSD, $P < 0.05$, Table 1). Cell biovolume of the two temperate
280 microalgae was the largest under HL and the smallest under LL, with an intermediary
281 biovolume for ML grown cultures.

282 The Chl *a* and Car contents of the two Arctic strains were lower than those of their
283 temperate counterparts under LL, ML, and HL conditions. Furthermore, the Chl *a*
284 content of the two temperate species significantly decreased under higher light
285 intensities (ML, HL, Tukey's HSD, $P < 0.05$, Fig. 2-atrazine concentration = $0 \mu\text{g L}^{-1}$),

286 while both Arctic species were unchanged under LL compared to ML and HL conditions.
287 The Car content of the two temperate species increased significantly under high light
288 intensity (ML and HL), while the two Arctic microalgae were not affected (Tukey's
289 HSD, $P < 0.05$, Fig. 2). In addition, except for T-MB, we found higher ROS levels in
290 microalgae grown under HL relative to the other two lower light conditions (LL and
291 ML) (Fig. 3-atrazine concentration = $0 \mu\text{g L}^{-1}$, Tukey's HSD, $P < 0.05$), and the ROS
292 contents of T-CN, A-CN, and A-MP of HL grown cultures were 1.2, 2.3, and 1.4 times
293 higher than those grown under LL, respectively.

294 3.1.2 Photosynthesis and energy dissipation processes

295 The maximum PSII quantum yield (Φ_M) of all studied species significantly
296 decreased with increasing growth light intensity and Φ_M of the two Arctic microalgae
297 declined more than that of their temperate counterparts (Tukey's HSD, $P > 0.05$, Table
298 1). A similar trend was observed with the operational PSII quantum yield (Φ'_M), but the
299 amplitudes of the declines were higher than for Φ_M ; except for A-MP showing no
300 alteration from LL to ML (Table 1). Together with the reduction of Φ_M and Φ'_M , the
301 maximum light efficiency usage (α) showed a decreasing trend with increasing light
302 intensity (Tukey's HSD, $P < 0.05$, Table 1). Furthermore, the maximum electron
303 transport rates ($r\text{ETR}_{\text{max}}$) and the light saturation coefficient (E_k) of Arctic and
304 temperate diatoms (T-CN and A-CN) increased significantly from LL to ML (except for
305 E_k of T-CN) and remarkably decreased from ML to HL (Tukey's HSD, $P < 0.05$, Table
306 1). Under the same condition, the E_k of Arctic and temperate green algae of *Micromonas*
307 (T-MB and A-MP) demonstrated similar trends, but no significant difference (Tukey's
308 HSD, $P > 0.05$, Table 1). Moreover, the maximal ability for dissipation of excess energy
309 (NPQ_{max}) of T-MB and A-MP also significantly increased from LL to ML, and markedly
310 decreased from ML to HL conditions (Tukey's HSD, $P < 0.05$, Table 1). However, the
311 NPQ_{max} of T-CN and A-CN increased significantly when the growth light intensity was
312 high (LL to ML and HL, Tukey's HSD, $P < 0.05$, Table 1). In addition, we observed
313 that the parameters Φ'_M , Φ_M , α , $r\text{ETR}_{\text{max}}$, and E_k for the two Arctic species were, to
314 different degrees, lower than those of their temperate counterparts under the different

315 growth light intensities.

316 3.1.3 Photosystem II energy fluxes

317 The energy conservation parameter of PI_{ABS} significantly decreased for all species,
318 except for A-CN, with increasing the growth light intensity (Tukey's HSD, $P < 0.05$,
319 Fig. 4). The PI_{ABS} of the two Arctic microalgae was less affected than their temperate
320 counterparts. The reduction in PI_{ABS} was also reflected in the decrease of electron
321 transport per active reaction center (ET_0/RC) for all studied species when the growth
322 light intensity was enhanced. The effective dissipation per active RC (DI_0/RC) of the
323 two temperate microalgae (T-CN and T-MB) was increased up to 252% and 224% from
324 LL to HL (Tukey's HSD, $P < 0.05$). This was accompanied by an increase in the
325 absorbed flux per active reaction center (ABS/RC) as an indicator of the PSII antenna
326 size. In contrast, DI_0/RC and ABS/RC in two Arctic microalgae did not significantly
327 change when the algae were grown under different light intensities (Tukey's HSD, $P >$
328 0.05 , Fig. 4). The maximal rate at which excitons were trapped by the active RCs
329 (TR_0/RC) was not affected by changes in growth light intensity. Furthermore, the PQ
330 pool size participating in the electron transport (qPQ) and non-photochemical
331 quenching (qE_{max}) were significantly increased in the two Arctic microalgae under HL,
332 compared to ML and LL (Tukey's HSD, $P < 0.05$, Fig. 4). In contrast, the qPQ and qE_{max}
333 of the two temperate species significantly decreased with increasing light intensity.

334 **3.2 Effects of atrazine and simazine on the ecophysiological characteristics of** 335 **Arctic and temperate species**

336 3.2.1 Growth rate, cell biovolume, pigment content, and ROS content

337 The growth rates of Arctic species (A-CN and A-MP) and their temperate
338 counterparts (T-CN and T-MB) significantly decreased after 72 h exposure to atrazine
339 or simazine independently of the growth light intensity (Tukey's HSD, $P < 0.05$, Fig.
340 1). Interestingly, although that trend was similar among the various light intensities, the
341 effect was stronger under the lowest light intensity. Moreover, the impact of the
342 herbicides on the growth rate for Arctic species was stronger than that of their temperate

343 counterparts when light intensity was enhanced. Although these herbicides inhibited the
344 growth of microalgae, the cell biovolume of the four studied species did not
345 significantly change for any tested conditions (Tukey's HSD, $P > 0.05$, Fig. S1), except
346 for T-MB and A-MP at high concentrations (100 and 250 $\mu\text{g/L}$) under ML and HL
347 conditions.

348 Chl *a* and Car contents did not change significantly at low concentrations of
349 atrazine and simazine ($\leq 25 \mu\text{g/L}$, Tukey's HSD, $P > 0.05$, Fig. 2), but declined
350 significantly at high concentrations ($> 25 \mu\text{g/L}$). The maximum reduction was observed
351 under HL compared to the other two low light intensities (LL and ML). Despite a
352 decreasing trend in Chl *a* and Car, the ratio of Car/Chl *a* remained unchanged (Tukey's
353 HSD, $P > 0.05$). ROS levels significantly increased with atrazine concentrations for
354 each light condition (LL, ML, and HL) (Tukey's HSD, $P < 0.05$). Although this trend
355 was similar among light intensities, the effect was stronger under HL (Fig. 3). The ROS
356 content also significantly increased with increasing simazine concentrations, and its
357 effect was greater for higher light intensities (data not shown).

358 3.2.2 Photosynthesis and energy dissipation processes

359 The operational PSII quantum yield (Φ'_M) of the four studied species significantly
360 decreased (Tukey's HSD, $P < 0.05$, Fig. 5) with increasing atrazine and simazine
361 concentrations for each growth light condition. Moreover, both Φ_M and Φ'_M of A-CN
362 decreased more than that of T-CN. In contrast, Φ_M and Φ'_M of A-MP decreased less
363 than that of T-MB except for low atrazine concentrations under LL ($< 25 \mu\text{g/L}$, Tukey's
364 HSD, $P < 0.05$, Fig. 5). The evaluated $\Phi'_M\text{-EC}_{50}$ of T-CN for atrazine under LL, ML,
365 and HL conditions were respectively 2.4, 1.7 and 1.8 times higher than those obtained
366 for A-CN (Table 1). Similar results were obtained for simazine. Both *Chaetoceros*
367 species have the lowest $\Phi'_M\text{-EC}_{50}$ (respectively 90 $\mu\text{g L}^{-1}$ and 28 $\mu\text{g L}^{-1}$ for the
368 temperate and Arctic species) for simazine under HL compared to LL and ML (Table
369 1). $\Phi'_M\text{-EC}_{50}$ of T-MB was equal to or higher than those of A-MP under LL, ML, and
370 HL conditions for atrazine. The highest simazine $\Phi'_M\text{-EC}_{50}$ evaluated for A-MP under
371 HL conditions (206 $\mu\text{g L}^{-1}$) was 4.2 times higher than that of T-MB (Table 1). The

372 parameter of Φ'_M was more sensitive than Φ_M in response to the herbicides. The energy
373 conservation parameter (PI_{ABS}) also decreased after exposure to $50 \mu\text{g L}^{-1}$ atrazine and
374 simazine under each light condition, but to a different extent than Φ_M and Φ'_M
375 depending on the tested species (Table 2). Non-photochemical quenching (qE_{max}) of the
376 four studied species was also significantly reduced with the addition of $50 \mu\text{g L}^{-1}$ of
377 atrazine under LL ML, and HL conditions (Tukey's HSD, $P < 0.05$, Table 2).

378 **3.3 Effects of growth light intensity on atrazine toxicity**

379 Because the effect of growth light intensity on simazine was similar to that of
380 atrazine, and because atrazine is detected more frequently than simazine in water bodies,
381 we mainly focus on atrazine for this section. Atrazine and ML alone significantly
382 reduced PI_{ABS} of T-CN by 98% and 95%, respectively, while their combined action was
383 less effective (71% inhibition) (Tukey's HSD, $P < 0.05$). Similar results were observed
384 for HL (Table 2). This trend was also observed among the other studied species (A-CN,
385 T-MB, and A-MP). Both Arctic species increased their non-photochemical quenching
386 (qE_{max}) to varying degrees (18-89%) under ML and HL growth conditions compared to
387 LL (Table 2). The combined effect of atrazine and ML decreased qE_{max} by 60% and 58%
388 respectively in A-CN and A-MP (Table 2). Furthermore, the combined effect of atrazine
389 and ML on the two temperate species only reduced qE_{max} by 14% for T-MB and 63%
390 for T-CN compared to ML exposure alone (27% and 72% reduction), and the combined
391 effect of atrazine and HL decreased more qE_{max} than the combination of atrazine and
392 ML condition (Table 2). The treatment with atrazine alone significantly induced the
393 production of ROS, but the combined effect of atrazine and ML or HL downregulated
394 the production of ROS (Table 2). According to Fig. 6, the removal of atrazine was
395 stronger under high light growth (HL) compared to the other two low light intensities
396 (LL and ML) except for T-CN (Tukey's HSD, $P < 0.05$). The removal ability of atrazine
397 by A-CN was higher than that of T-CN under LL, ML and HL conditions. Meanwhile,
398 the A-MP showed higher removal ability of atrazine compared to T-MB under ML and
399 HL conditions except for LL condition.

401 **4 Discussion**

402 **4.1 Influence of growth light intensity on Arctic microalgae and their temperate** 403 **counterparts**

404 **4.1.1 Photoadaptation processes**

405 Light adaptation processes developed by microalgae allow them to thrive in low or
406 high light environments by modulating their eco-physiological properties (Agarwal et
407 al. 2019, Young and Schmidt 2020). In our experiments, high light induced similar
408 photophysiological responses among the studied species. Growth under higher (but not
409 excessive) light intensity led to a significant increase in growth rates, which may be
410 attributed to the Chl *a*/C evolution with changes in light intensity (Croteau et al. 2022,
411 Lacour et al. 2018). The reduction of Chl *a* in all species after HL photoadaptation was
412 typically seen as a result of lower light absorption as would be expected given that light
413 absorption is positively related to cellular Chl *a* content (MacIntyre et al. 2002).
414 Increase in Car may play a role in protecting the photosynthetic apparatus under high
415 light intensities. Indeed, either directly or indirectly, these pigments are involved in
416 scavenging ROS (Sedoud et al. 2014). Furthermore, the slight but significant increase
417 of the light harvesting antenna size of all studied species following HL adaptation
418 indicated a relatively low photochemically effective cross-section to reduce the chance
419 of photons entering the photosynthetic electron transport chain to avoid photo-damage
420 (Finkel et al. 2010). These modifications observed under high light conditions
421 minimized the excitation pressure on the photosynthetic apparatus despite the increased
422 light availability (Agarwal et al. 2019). Non-photochemical quenching (NPQ) (the main
423 component-qE) is known to be an efficient photoprotective mechanism (Goss and
424 Lepetit 2015). The higher intrinsic NPQ_{max} of the studied Arctic species under HL, as
425 compared to LL and ML conditions, may indicate that this process is activated to reduce
426 PSII damage (Kirilovsky 2015). Indeed, light intensity above the photosynthesis
427 saturation point (E_k over $400 \mu\text{mol photons m}^{-2} \text{ s}^{-1}$, Table 1) can increase ROS
428 production (Metsoviti et al. 2019), which was consistent with the reduced
429 photosynthetic efficiency (Φ_M and Φ'_M) under HL. Therefore, the observed high ROS

430 content inducing inactivation of PSII under HL as compared to ML and LL, indicates
431 that cellular defense strategies were not sufficient to deal with photochemical damage
432 and oxidative stress.

433 **4.1.2 Differences between Arctic and temperate microalgae**

434 The observed low Chl *a* could be responsible for the lower photosynthetic
435 efficiency (Φ_M and Φ'_M) in both Arctic species compared to their temperate
436 counterparts under all light conditions since Chl *a* is proportional to the number of
437 photosynthetic systems (MacIntyre et al. 2002). Some authors have shown that the A-
438 MP had only half the content of active PSII reaction centers compared to T-MB (Ni et
439 al. 2017). This is also confirmed by the low performance index of photons (PI_{ABS}),
440 showing the low photosynthetic efficiency. Furthermore, a small amount of Chl *a* is
441 usually present in Arctic species growing under light-limiting conditions to avoid
442 stacking effects between chlorophylls (Yan et al. 2018). As a result, the absence of
443 markedly reduced Chl *a* content in HL-adapted Arctic cells compared with LL-adapted
444 cells suggested that they did not possess the same light-modulating ability as temperate
445 microalgae. Temperate microalgae usually decrease their light absorption at high
446 irradiance levels by reducing Chl *a* associated with their light-harvesting complexes, as
447 observed in both temperate species studied here (decreased Chl *a* under HL, Fig. 2).
448 Interestingly, qPQ , which reflects the plastoquinone (PQ) pool size participating in the
449 electron transport (Xu et al. 2019), significantly increased in the two Arctic species
450 under HL, indicating that increased electron supply to the PQ pool was satisfied by
451 increasing the ability to transfer energy away from PSII, and accompanied by high
452 dissipation capacity (higher qE_{max}) (Fig. 4). In comparison, temperate species had
453 reduced qPQ and lower qE_{max} under HL. The redox state of the PQ pool plays an
454 important role in light adaptation of algae and regulation of gene expression in the
455 chloroplasts and nucleus under varying light conditions (Lepetit et al. 2013, Virtanen et
456 al. 2021). In summary, the photoadaptation strategies between temperate and Arctic
457 microalgae show different extents. Arctic microalgae appear to mainly rely on increased
458 PQ pool size and strong dissipation capacity (qE_{max}) to cope with higher light intensity,

459 whereas their temperate counterparts appear to mainly rely on the reduction of pigments
460 associated with light-harvesting complex (LHC) to regulate light absorption. In
461 addition, we observed substantial differences in the adaptation capacity of the two
462 microalgal classes. The diatoms had higher growth rate (μ), higher light efficiency use
463 (α) and higher photosynthetic electron transfer rate ($rETR_{max}$) relative to the green
464 microalgae, exhibiting their high photoadaptation capacity to change in ambient light
465 intensity (Table 1). This mechanism concurs with the dominance of diatoms in the
466 seasonally changing Arctic Ocean (Croteau et al. 2022, Wolf et al. 2018).

467 **4.2 Effects of atrazine and simazine on Arctic microalgae and their temperate** 468 **counterparts under each light condition**

469 Based on the EC_{50} of Φ_M and Φ'_M (Table 1), temperate *C. neogracile* was more
470 tolerant to atrazine and simazine than Arctic *C. neogracilis* under all light conditions,
471 while Arctic *M. polaris* was less affected by these herbicides than temperate *M. bravo*,
472 and the sensitivity sequence was T-CN<A-CN<A-MP<T-MP. We found that atrazine
473 was more toxic than simazine in all studied species under all light conditions even
474 though they had the same mode of action. This higher toxicity was attributed to the high
475 $\log K_{OW}$ of atrazine resulting in a high affinity for the herbicide binding site (Ronka
476 2016). Atrazine and simazine, as photosynthetic inhibitor herbicides, can bind to the
477 Q_B site of the D1 protein in PSII (Bai et al. 2015). Therefore, the observed inhibition of
478 photosynthetic electron transport chains (decreased Φ'_M) in the Arctic and temperate
479 species was observed in the presence of these herbicides, which was also evidenced by
480 lower electron transfer per active RC (ET_0/RC). The transthylakoidal proton gradient
481 required to activate non-photochemical quenching (qE) (Cao et al. 2013) was also
482 reduced by inhibiting electron transport. As a result, the microalgae reduced thermal
483 dissipation capacity (qE_{max}) under herbicide exposure preventing the efficient
484 dissipation of excess energy. Therefore, the organisms underwent higher excitation
485 pressure on PSII due to blocked electron transport, resulting in the production of large
486 ROS concentrations (Fig. 3), which can eventually deactivate PSII RC (Gomes and
487 Juneau 2017, Sun et al. 2020). This is in accordance with the increased effective antenna

488 size of active RC (ABS/RC), showing a strong decrease in the active PSII RC
489 population as previously demonstrated under cadmium and high light stress (Du et al.
490 2019). The reduction of active PSII RCs induced by ROS may explain the decreased
491 photochemistry efficiency of PSII (Φ_M), which was ultimately reflected in the growth
492 inhibition of all studied species under the different light conditions. This observation
493 was consistent with previous studies showing that photosynthesis inhibitor herbicides
494 (diuron and Irgarol) inhibit the growth of freshwater microalgae (Kottuparambil et al.
495 2017). In addition, the reduction of Chl *a* in all species (Fig. 2) was attributed to the
496 continuous accumulation of ROS in the presence of atrazine or simazine (Almeida et
497 al. 2017). Atrazine and simazine disturbed the balance between light absorption and
498 energy utilization, since PI_{ABS} , as an indicator for energy conservation from photons
499 absorbed by PSII to intersystem electron acceptors, significantly decreased irrespective
500 of growth light intensity (Sun et al. 2020).

501 **4.3 Combined effects of growth light intensity and atrazine on Arctic microalgae** 502 **and their temperate counterparts**

503 Significant interactions between growth light intensity and atrazine were observed
504 for growth, Φ_M , Φ'_M , and PI_{ABS} ($P < 0.0001$). Atrazine was chosen to describe the
505 interaction with light since the obtained results for simazine were similar due to their
506 same mode of action. According to the EC_{50} of Φ_M and Φ'_M , all studied species were
507 more affected by atrazine under HL compared to the other lower light intensities (LL
508 and ML) (Table 1). Although atrazine and light alone, respectively, decreased the light
509 energy conversion (PI_{ABS}), interestingly it appears that the combination of HL and
510 herbicides reversed this effect on PI_{ABS} (Table 2). This indicates that photoadaptation
511 processes, such as changes in pigments, mitigate the effects of herbicides on light
512 energy conversation. Indeed, lower Chl *a* in both Arctic species and higher Car
513 concentration in both temperate species may decrease, respectively, light absorption
514 and ROS scavenging, which help to protect the photosystem apparatus. The combined
515 inhibitory effect was small in tolerant species (T-CN and A-MP) to atrazine compared
516 to the sensitive species (A-CN and T-MB). Changes in PSII photochemistry are

517 frequently related to the modifications of the energy dissipation pathway (qE_{\max}) (Du
518 et al. 2019). The combined effect of HL and atrazine ($50 \mu\text{g L}^{-1}$, concentration near the
519 EC_{50} for most species) on the thermal dissipation ability (qE_{\max}) of Arctic species was
520 greater than the effects of atrazine alone, although high qE_{\max} was already induced after
521 HL adaptation without herbicide. While the effect of qE_{\max} was slight in temperate
522 species under the combined conditions of HL and atrazine, HL and atrazine alone
523 considerably decreased qE_{\max} (Table 2). Therefore, we can suggest that other parts of
524 the non-photochemical energy dissipation process (qT or qI) in temperate species were
525 highly effective under HL adaptation since some authors have shown that qE was in
526 general much lower on green microalgae than in diatoms since qT is more important
527 than qE in green algae of *Chlamydomonas* (Allorent et al. 2013). These results showed
528 that qE_{\max} , as an indicator of the thermal dissipation capacity, was less indicative than
529 Φ'_M and PI_{ABS} , probably because the later integrated the effects of the herbicide and HL
530 on the photosynthetic electron transport and the related energy dissipation processes,
531 while qE_{\max} only represents one of the components of NPQ. This is in accordance with
532 a recent study showing that the performance index PI_{ABS} was a more convincing
533 indicator of atrazine toxicity compared to growth rate and Φ_{E0} (Sun et al. 2020). On the
534 other hand, the combination of HL effect and $50 \mu\text{g L}^{-1}$ atrazine of microalgae mitigated
535 the ROS burst (Table 2), which was attributed to the increased non-photochemical
536 quenching (NPQ_{\max}) after HL adaptation to dissipate excess energy to reduce the
537 excitation pressure on PSII (Silva et al. 2021). Furthermore, with the exception of T-
538 CN, the removal of atrazine by microalgae increased with increasing culture light
539 intensity (LL-ML-HL), which can largely explain the high herbicide toxicity under HL
540 intensity. We hypothesize that high light condition induces higher uptake of pesticides
541 as it was previously demonstrated for other contaminants such as metals (Du et al. 2019).
542 As a result, we can assume that even the effective induction of photosynthetic defense
543 measures (NPQ and Car content) upon HL adaptation was unable to deal with the
544 combination of higher light intensity and herbicides. Interestingly, the growth inhibition
545 caused by atrazine of temperate species grown under HL was alleviated more than the
546 cells grown under LL and ML (Fig. 1). This can be explained that temperate microalgae

547 can effectively utilize the absorbed light energy and perform reasonable energy
548 allocation (high α and PI_{ABS} , Table 1) for carbon fixation. However, Arctic microalgae
549 grown under HL were unable to prevent growth inhibition caused by atrazine due to the
550 observed inefficient capacity for light absorption and light energy conversion (Fig. 4).

551 **4.4 Concluding remarks**

552 We demonstrated that the extent of light-adaption responses between Arctic and
553 temperate microalgae were different, these differences can influence the toxicity of
554 atrazine, and probably other contaminants. Furthermore, the microalgal protection
555 measures of NPQ and Car (photoprotective pigment) after HL adaptation were
556 insufficient to handle the combined impacts of high light intensity and atrazine stress,
557 as atrazine removal ability was enhanced with increasing growth light intensity. Our
558 results indicated that light plays a non-negligible role in regulating the toxicity of
559 herbicide for microalgae. We recommend that variation in light intensities should be
560 considered in herbicide risk assessments for Arctic and temperate ecosystems, because
561 of its role in affecting photoprotective strategies and atrazine removal.

562 **Acknowledgments**

563 This work was supported by a DFO grant (MECTS-#3789712) obtained by Philippe
564 Juneau, Johann Lavaud, and Beatrix Beisner, and the Natural Science and Engineering
565 Research Council of Canada (NSERC) (RGPIN-2017-06210) awarded to Philippe
566 Juneau. The authors thanks also the GRIL (Groupe de recherche interuniversitaire en
567 limnologie) for funding to PJ and BEB that supported Juan Du's Ph.D.

568

569 **References**

- 570 Agarwal, A., Patil, S., Gharat, K., Pandit, R.A. and Lali, A.M. (2019) Modulation in
571 light utilization by a microalga *Asteracys* sp. under mixotrophic growth regimes.
572 *Photosynthesis Research* 139(1-3), 553-567.
- 573 Allorement, G., Tokutsu, R., Roach, T., Peers, G., Cardol, P., Girard-Bascou, J.,
574 Seigneurin-Berny, D., Petroustos, D., Kuntz, M., Breyton, C., Franck, F., Wollman, F.A.,
575 Niyogi, K.K., Krieger-Liszkay, A., Minagawa, J. and Finazzi, G. (2013) A dual strategy
576 to cope with high light in *Chlamydomonas reinhardtii*. *Plant Cell* 25(2), 545-557.
- 577 Almeida, A.C., Gomes, T., Langford, K., Thomas, K.V. and Tollefsen, K.E. (2017)
578 Oxidative stress in the algae *Chlamydomonas reinhardtii* exposed to biocides. *Aquatic*
579 *Toxicology* 189, 50-59.
- 580 Bai, X., Sun, C., Xie, J., Song, H., Zhu, Q., Su, Y., Qian, H. and Fu, Z. (2015) Effects
581 of atrazine on photosynthesis and defense response and the underlying mechanisms in
582 *Phaeodactylum tricorutum*. *Environmental Science and Pollution Research* 22(17),
583 499-507.
- 584 Balzano, S., Marie, D., Gourvil, P. and Vaultot, D. (2012) Composition of the summer
585 photosynthetic pico and nanoplankton communities in the Beaufort Sea assessed by T-
586 RFLP and sequences of the 18S rRNA gene from flow cytometry sorted samples. *ISME*
587 *Journal* 6(8), 1480-1498.
- 588 Balzano, S., Percopo, I., Siano, R., Gourvil, P., Chanoine, M., Marie, D., Vaultot, D. and
589 Sarno, D. (2017) Morphological and genetic diversity of Beaufort Sea diatoms with
590 high contributions from the *Chaetoceros neogracilis* species complex. *J Phycol* 53(1),
591 161-187.
- 592 Baxter, L., Brain, R.A., Lissemore, L., Solomon, K.R., Hanson, M.L. and Prosser, R.S.
593 (2016) Influence of light, nutrients, and temperature on the toxicity of atrazine to the
594 algal species *Raphidocelis subcapitata*: Implications for the risk assessment of
595 herbicides. *Ecotoxicology and Environmental Safety* 132, 250-259.
- 596 Bellacicco, M., Volpe, G., Colella, S., Pitarch, J. and Santoleri, R. (2016) Influence of
597 photoacclimation on the phytoplankton seasonal cycle in the Mediterranean Sea as seen
598 by satellite. *Remote Sensing of Environment* 184, 595-604.
- 599 Bilger, W. and Björkman, O. (1990) Role of the xanthophyll cycle in photoprotection
600 elucidated by measurements of light-induced absorbance changes, fluorescence and
601 photosynthesis in leaves of *Hedera canariensis*. *Photosynthesis Research* 25(3), 173-
602 185.
- 603 Cao, S., Zhang, X., Xu, D., Fan, X., Mou, S., Wang, Y., Ye, N. and Wang, W. (2013) A
604 transthylakoid proton gradient and inhibitors induce a non-photochemical fluorescence
605 quenching in unicellular algae *Nannochloropsis* sp. *FEBS Letters* 587(9), 1310-1315.
- 606 Chalifour, A. and Juneau, P. (2011) Temperature-dependent sensitivity of growth and
607 photosynthesis of *Scenedesmus obliquus*, *Navicula pelliculosa* and two strains of
608 *Microcystis aeruginosa* to the herbicide atrazine. *Aquatic Toxicology* 103(1-2), 9-17.
- 609 Chalifour, A., LeBlanc, A., Sleno, L. and Juneau, P. (2016) Sensitivity of *Scenedesmus*
610 *obliquus* and *Microcystis aeruginosa* to atrazine: effects of acclimation and mixed
611 cultures, and their removal ability. *Ecotoxicology* 25(10), 1822-1831.

- 612 Chen, S., Chen, M., Wang, Z., Qiu, W., Wang, J., Shen, Y., Wang, Y. and Ge, S. (2016)
613 Toxicological effects of chlorpyrifos on growth, enzyme activity and chlorophyll a
614 synthesis of freshwater microalgae. *Environmental Toxicology and Pharmacology* 45, 179-
615 186.
- 616 Croteau, D., Lacour, T., Schiffrine, N., Morin, P.I., Forget, M.H., Bruyant, F., Ferland,
617 J., Lafond, A., Campbell, D.A., Tremblay, J.É., Babin, M. and Lavaud, J. (2022) Shifts
618 in growth light optima among diatom species support their succession during the spring
619 bloom in the Arctic. *Journal of Ecology*.
- 620 Dar, G.H., Hakeem, K.R., Mehmood, M.A. and Qadri, H. (2021) *Freshwater Pollution
621 and Aquatic Ecosystems: Environmental Impact and Sustainable Management*. CRC
622 Press.
- 623 Deblois, C.P., Dufresne, K. and Juneau, P. (2013a) Response to variable light intensity
624 in photoacclimated algae and cyanobacteria exposed to atrazine. *Aquatic Toxicology*
625 126, 77-84.
- 626 Deblois, C.P., Marchand, A. and Juneau, P. (2013b) Comparison of photoacclimation in
627 twelve freshwater photoautotrophs (chlorophyte, bacillaryophyte, cryptophyte and
628 cyanophyte) isolated from a natural community. *PLoS One* 8(3), e57139.
- 629 DeLorenzo, M.E. (2001) toxicity of pesticides to aquatic microorganisms: a review.
630 *Environmental Toxicology and Chemistry* 20 (1), 84-98.
- 631 Dong, H.P., Dong, Y.L., Cui, L., Balamurugan, S., Gao, J., Lu, S.H. and Jiang, T. (2016)
632 High light stress triggers distinct proteomic responses in the marine diatom
633 *Thalassiosira pseudonana*. *BMC Genomics* 17(1), 994.
- 634 Du, J., Qiu, B., Pedrosa Gomes, M., Juneau, P. and Dai, G. (2019) Influence of light
635 intensity on cadmium uptake and toxicity in the cyanobacteria *Synechocystis* sp.
636 PCC6803. *Aquatic Toxicology* 211, 163-172.
- 637 Dubinsky, Z. and Stambler, N. (2009) Photoacclimation processes in phytoplankton:
638 mechanisms, consequences, and applications. *Aquatic Microbial Ecology* 56, 163-176.
- 639 Dupraz, V., Coquille, N., Menard, D., Sussarellu, R., Hauguarreau, L. and Stachowski-
640 Haberkorn, S. (2016) Microalgal sensitivity varies between a diuron-resistant strain and
641 two wild strains when exposed to diuron and irgarol, alone and in mixtures.
642 *Chemosphere* 151, 241-252.
- 643 Edwards, K.F., Thomas, M.K., Klausmeier, C.A. and Litchman, E. (2015) Light and
644 growth in marine phytoplankton: allometric, taxonomic, and environmental variation.
645 *Limnology and Oceanography* 60(2), 540-552.
- 646 Eilers, P.H.C. and Peeters, J.C.H. (1988) A model for the relationship between light
647 intensity and the rate of photosynthesis in phytoplankton. *Ecological Modelling* 42(3-
648 4), 199-215.
- 649 Finkel, Z.V., Beardall, J., Flynn, K.J., Quigg, A., Rees, T.A.V. and Raven, J.A. (2010)
650 Phytoplankton in a changing world: cell size and elemental stoichiometry. *Journal of
651 Plankton Research* 32(1), 119-137.
- 652 Genty, B., Briantais, J.M. and Baker, N.R. (1989) The relationship between the quantum
653 yield of photosynthetic electron transport and quenching of chlorophyll fluorescence.
654 *Biochimica et Biophysica Acta* 990(1), 87-92.
- 655 Gomes, M.P. and Juneau, P. (2017) Temperature and Light Modulation of Herbicide

- 656 Toxicity on Algal and Cyanobacterial Physiology. *Frontiers in Environmental Science*
657 5.
- 658 Goss, R. and Lepetit, B. (2015) Biodiversity of NPQ. *Journal of Plant Physiology* 172,
659 13-32.
- 660 Guillard, R.R.L. and Hargraves, P.E. (1993) *Stichochrysis immobilis* is a diatom, not a
661 chrysophyte. *Phycologia* 32(3), 234-236.
- 662 Handler, E. (2017) Responses to Light Intensity and Regimes by an Arctic strain of the
663 picophytoplankton *Micromonas* CCMP2099.
- 664 Hopes, A. and Mock, T. (2015) eLS, pp. 1-9.
- 665 Jeffrey, S.W. and Humphrey, G.F. (1975) New spectrophotometric equations for
666 determining chlorophylls a, b, c1 and c2 in higher plants, algae and natural
667 phytoplankton. *Biochemie und Physiologie der Pflanzen* 167(2), 191-194.
- 668 Jiang, H.X., Chen, L.S., Zheng, J.G., Han, S., Tang, N. and Smith, B.R. (2008)
669 Aluminum-induced effects on Photosystem II photochemistry in Citrus leaves assessed
670 by the chlorophyll a fluorescence transient. *Tree Physiology* 28(12), 1863-1871.
- 671 Juneau, P., David, D. and Saburo, M. (2001) Evaluation of different algal species
672 sensitivity to mercury and metolachlor by PAM-fluorometry. *Chemosphere* 45(4-5),
673 589-598.
- 674 Kirilovsky, D. (2015) Modulating energy arriving at photochemical reaction centers:
675 orange carotenoid protein-related photoprotection and state transitions. *Photosynthesis*
676 *Research* 126(1), 3-17.
- 677 Kottuparambil, S., Brown, M.T., Park, J., Choi, S., Lee, H., Choi, H.G., Depuydt, S.
678 and Han, T. (2017) Comparative assessment of single and joint effects of diuron and
679 Irgarol 1051 on Arctic and temperate microalgae using chlorophyll a fluorescence
680 imaging. *Ecological Indicators* 76, 304-316.
- 681 Lacour, T., Babin, M. and Lavaud, J. (2020) Diversity in xanthophyll cycle pigments
682 content and related nonphotochemical quenching (NPQ) among microalgae:
683 implications for growth strategy and ecology. *Journal of Phycology* 56(2), 245-263.
- 684 Lacour, T., Larivière, J., Ferland, J., Bruyant, F., Lavaud, J. and Babin, M. (2018) The
685 Role of Sustained Photoprotective Non-photochemical Quenching in Low Temperature
686 and High Light Acclimation in the Bloom-Forming Arctic Diatom *Thalassiosira*
687 *gravida*. *Frontiers in Marine Science* 5.
- 688 Lepetit, B., Gelin, G., Lepetit, M., Sturm, S., Vugrinec, S., Rogato, A., Kroth, P.G.,
689 Falciatore, A. and Lavaud, J. (2017) The diatom *Phaeodactylum tricorutum* adjusts
690 nonphotochemical fluorescence quenching capacity in response to dynamic light via
691 fine-tuned Lhcx and xanthophyll cycle pigment synthesis. *New Phytologist* 214(1),
692 205-218.
- 693 Lepetit, B., Sturm, S., Rogato, A., Gruber, A., Sachse, M., Falciatore, A., Kroth, P.G.
694 and Lavaud, J. (2013) High light acclimation in the secondary plastids containing
695 diatom *Phaeodactylum tricorutum* is triggered by the redox state of the plastoquinone
696 pool. *Plant physiology* 161(2), 853-865.
- 697 Leu, E., Wiktor, J., Søreide, J.E., Berge, J. and Falk-Petersen, S. (2010) Increased
698 irradiance reduces food quality of sea ice algae. *Marine Ecology Progress Series* 411,
699 49-60.

- 700 MacIntyre, H.L., Todd, M.K. and Todd, H.K. (2002) PHOTOACCLIMATION OF
701 PHOTOSYNTHESIS IRRADIANCE RESPONSE CURVES AND
702 PHOTOSYNTHETIC. *Journal of Phycology*.
- 703 Metsoviti, M.N., Papapolymerou, G., Karapanagiotidis, I.T. and Katsoulas, N. (2019)
704 Effect of Light Intensity and Quality on Growth Rate and Composition of *Chlorella*
705 *vulgaris*. *Plants (Basel)* 9(1).
- 706 Ni, G., Zimbalatti, G., Murphy, C.D., Barnett, A.B., Arsenault, C.M., Li, G., Cockshutt,
707 A.M. and Campbell, D.A. (2017) Arctic *Micromonas* uses protein pools and non-
708 photochemical quenching to cope with temperature restrictions on Photosystem II
709 protein turnover. *Photosynthesis Research* 131(2), 203-220.
- 710 Osborne, E., Richter-Menge, J. and Jeffries, M. (2018) Tundra greenness. Arctic Report
711 Card, 2018.
- 712 Pučko, M., Stern, G.A., Burt, A.E., Jantunen, L.M., Bidleman, T.F., Macdonald, R.W.,
713 Barber, D.G., Geilfus, N.X. and Rysgaard, S. (2017) Current use pesticide and legacy
714 organochlorine pesticide dynamics at the ocean-sea ice-atmosphere interface in resolute
715 passage, Canadian Arctic, during winter-summer transition. *Science of the Total*
716 *Environment* 580, 1460-1469.
- 717 Ronka, S. (2016) Removal of triazine-based herbicides on specific polymeric sorbent:
718 batch studies. *Pure and Applied Chemistry* 88(12), 1167-1177.
- 719 Schmale, J., Arnold, S.R., Law, K.S., Thorp, T., Anenberg, S., Simpson, W.R., Mao, J.
720 and Pratt, K.A. (2018) Local Arctic Air Pollution: A Neglected but Serious Problem.
721 *Earth's Future* 6(10), 1385-1412.
- 722 Sedoud, A., Lopez-Igual, R., Ur Rehman, A., Wilson, A., Perreau, F., Boulay, C., Vass,
723 I., Krieger-Liszky, A. and Kirilovsky, D. (2014) The Cyanobacterial Photoactive
724 Orange Carotenoid Protein Is an Excellent Singlet Oxygen Quencher. *Plant Cell* 26(4),
725 1781-1791.
- 726 Seoane, M., Gonzalez-Fernandez, C., Soudant, P., Huvet, A., Esperanza, M., Cid, A.
727 and Paul-Pont, I. (2019) Polystyrene microbeads modulate the energy metabolism of
728 the marine diatom *Chaetoceros neogracile*. *Environ Pollut* 251, 363-371.
- 729 Serodio, J. and Lavaud, J. (2011) A model for describing the light response of the
730 nonphotochemical quenching of chlorophyll fluorescence. *Photosynthesis Research*
731 108(1), 61-76.
- 732 Silva, F.B., Costa, A.C., Megguer, C.A., Lima, J.S., Batista, P.F., Martins, D.A.,
733 Almeida, G.M., Domingos, M. and Müller, C. (2021) Atrazine toxicity to handroanthus
734 heptaphyllus, a nontarget species from a Brazilian biome threatened by agriculture.
735 *Environmental Quality Management* 30(3), 17-25.
- 736 Stachowski-Haberkorn, S., Jerome, M., Rouxel, J., Khelifi, C., Rince, M. and Burgeot,
737 T. (2013) Multigenerational exposure of the microalga *Tetraselmis suecica* to diuron
738 leads to spontaneous long-term strain adaptation. *Aquatic Toxicology* 140-141, 380-
739 388.
- 740 Sun, C., Xu, Y., Hu, N., Ma, J., Sun, S., Cao, W., Klobucar, G., Hu, C. and Zhao, Y.
741 (2020) To evaluate the toxicity of atrazine on the freshwater microalgae *Chlorella* sp.
742 using sensitive indices indicated by photosynthetic parameters. *Chemosphere* 244,
743 125514.

- 744 Virtanen, O., Khorobrykh, S. and Tyystjarvi, E. (2021) Acclimation of *Chlamydomonas*
745 *reinhardtii* to extremely strong light. *Photosynthesis Research* 147(1), 91-106.
- 746 Vorkamp, K. and Riget, F.F. (2014) A review of new and current-use contaminants in
747 the Arctic environment: evidence of long-range transport and indications of
748 bioaccumulation. *Chemosphere* 111, 379-395.
- 749 Wagner, H., Jakob, T. and Wilhelm, C. (2006) Balancing the energy flow from captured
750 light to biomass under fluctuating light conditions. *New Phytologist* 169(1), 95-108.
- 751 Wolf, K.K.E., Hoppe, C.J.M. and Rost, B. (2018) Resilience by diversity: Large
752 intraspecific differences in climate change responses of an Arctic diatom. *Limnology*
753 *and Oceanography* 63(1), 397-411.
- 754 Xu, K., Racine, F., He, Z. and Juneau, P. (2019) Impacts of hydroxyphenylpyruvate
755 dioxygenase (HPPD) inhibitor (mesotrione) on photosynthetic processes in
756 *Chlamydomonas reinhardtii*. *Environmental Pollution* 244, 295-303.
- 757 Yan, D., Beardall, J. and Gao, K. (2018) Variation in cell size of the diatom
758 *Coscinodiscus granii* influences photosynthetic performance and growth.
759 *Photosynthesis Research* 137(1), 41-52.
- 760 Young, J.N. and Schmidt, K. (2020) It's what's inside that matters: physiological
761 adaptations of high-latitude marine microalgae to environmental change. *New*
762 *Phytologist* 227(5), 1307-1318.
- 763 Zhao, F., Li, Y., Huang, L., Gu, Y., Zhang, H., Zeng, D. and Tan, H. (2018) Individual
764 and combined toxicity of atrazine, butachlor, halosulfuron-methyl and mesotrione on
765 the microalga *Selenastrum capricornutum*. *Ecotoxicology and Environmental Safety*
766 148, 969-975.

767 Table 1. The effect of light intensity (LL, ML, and HL) on the growth rate, cell
768 biovolume, Φ_M , Φ'_M , α , $rETR_{max}$, E_k , and NPQ_{max} of temperate *C. neogracile* (T-CN),
769 *M. bravo* (T-MB), Arctic *C. neogracilis* (A-CN), and Arctic *M. polaris* (A-MP). EC_{50}
770 for the operational PSII quantum yield (Φ'_M) after 72 h exposure to atrazine and
771 simazine under three different light intensities (LL, ML, and HL). Strains in the same
772 column exposed to the different light intensity with different superscript letters (a-c)
773 were significantly different (Tukey's HSD, $P < 0.05$). The numbers in parentheses are
774 the percentages of the control values. Data expressed as means \pm SD ($n = 6$).
775

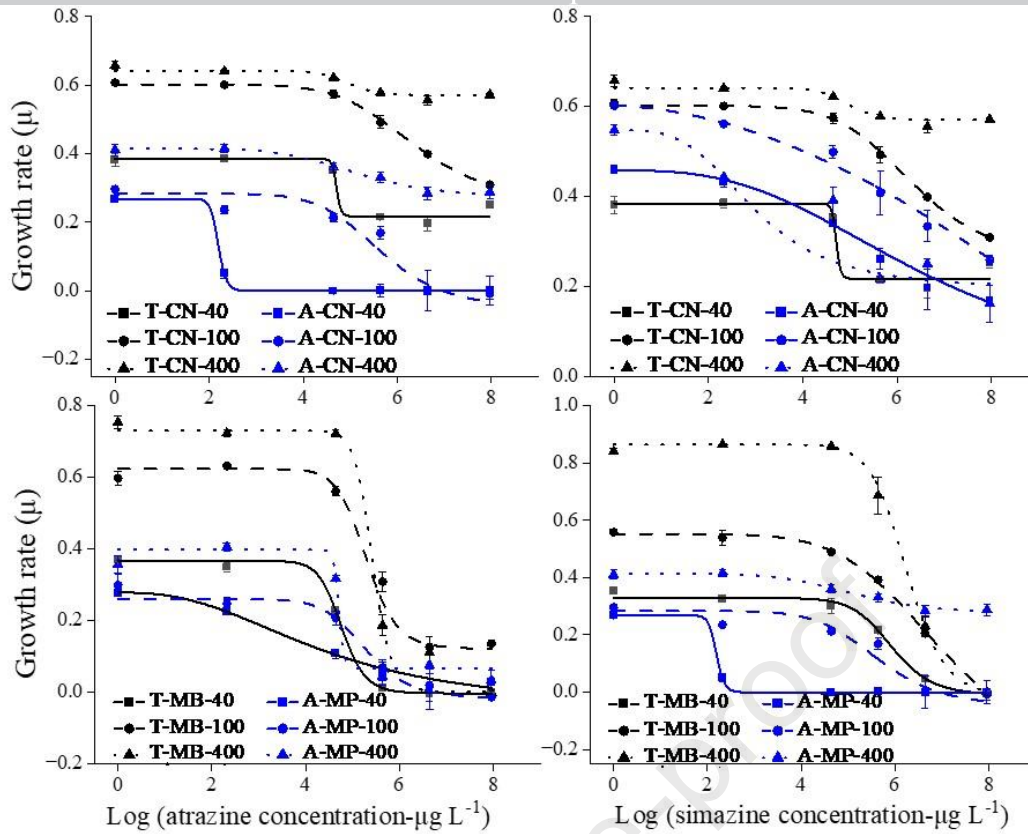
776

| Species | Light | Growth rate (μ) | Volume (μm^3) | Φ_M | Φ'_M | α | rETR _{max} | E_k | NPQ _{max} | EC ₅₀ ⁻ Φ'_M (Atra) (Sim) | |
|---------|-------|------------------------------|-------------------------------|-------------------------------|-------------------------------|--------------------------------|---------------------------|----------------------------|-----------------------------|---|---------|
| T-CN | LL | 0.37±0.02 (100) ^a | 114±8.89(100) ^a | 0.692±0.00 (100) ^a | 0.682±0.01 (100) ^a | 0.713±0.01 (100) ^a | 333±36 (100) ^a | 467±52 (100) ^a | 1.5±1.24 (100) ^a | 95±7.4 | 121±7.9 |
| | ML | 0.64±0.03 (170) ^b | 148±9.59(130) ^b | 0.647±0.00 (93) ^b | 0.646±0.00 (95) ^b | 0.665±0.01 (93) ^b | 421±17 (126) ^b | 633±23 (136) ^b | 1.3±0.24 (12) ^b | 66±1.4 | 142±6.7 |
| | HL | 0.66±0.02 (177) ^b | 164±4.88(144) ^c | 0.608±0.01 (88) ^c | 0.510±0.03 (75) ^c | 0.624±0.02 (88) ^c | 253±63 (76) ^c | 404±91 (87) ^a | 10±0.00 (105) ^a | 34±1.1 | 90±12 |
| A-CN | LL | 0.43±0.03 (100) ^a | 45±3.06 (100) ^a | 0.674±0.01 (100) ^a | 0.607±0.01 (100) ^a | 0.607±0.02 (100) ^a | 265±34 (100) ^a | 432±55 (100) ^a | 1.6±0.62 (100) ^a | 39±1.7 | 52±0.7 |
| | ML | 0.57±0.09 (131) ^b | 63±3.84 (140) ^b | 0.584±0.00 (87) ^b | 0.553±0.01 (91) ^b | 0.569±0.04 (94) ^a | 370±91 (140) ^b | 648±158 (150) ^b | 1.8±0.54 (113) ^a | 37±2.1 | 62±2.1 |
| | HL | 0.57±0.08 (130) ^b | 61±7.57 (136) ^b | 0.525±0.02 (78) ^c | 0.246±0.02 (41) ^c | 0.473±0.07 (78) ^b | 91±13 (34) ^c | 196±46 (45) ^c | 3.7±0.92 (231) ^b | 12±3.2 | 28±2.0 |
| T-MB | LL | 0.36±0.01 (100) ^a | 4±0.09 (100) ^a | 0.685±0.01 (100) ^a | 0.678±0.02 (100) ^a | 0.519±0.05 (100) ^{ab} | 247±61 (100) ^a | 369±162 (100) ^a | 1.5±0.01 (100) ^a | 36±5.9 | 61±7.0 |
| | ML | 0.58±0.03 (160) ^b | 5±0.00 (134) ^b | 0.647±0.00 (94) ^b | 0.562±0.00 (83) ^b | 0.597±0.01 (115) ^a | 244±25 (99) ^a | 430±48 (117) ^a | 1.9±0.11 (127) ^b | 31±2.3 | 32±1.8 |
| | HL | 0.80±0.05 (220) ^c | 5±0.19 (141) ^c | 0.598±0.01 (87) ^c | 0.357±0.01 (53) ^c | 0.499±0.07 (96) ^b | 180±31 (73) ^a | 368±82 (100) ^a | 1.3±0.33 (87) ^a | 30±4.8 | 49±1.4 |
| A-MP | LL | 0.27±0.01 (100) ^a | 5±0.05 (100) ^a | 0.675±0.02 (100) ^a | 0.505±0.02 (100) ^a | 0.445±0.09 (100) ^{ab} | 114±56 (100) ^a | 249±104 (100) ^a | 2.2±0.71 (100) ^a | 39±1.3 | 55±3.4 |
| | ML | 0.30±0.02 (109) ^b | 6±0.26 (102) ^a | 0.618±0.02 (92) ^b | 0.491±0.02 (97) ^a | 0.493±0.04 (111) ^a | 156±21 (137) ^a | 356±28 (143) ^a | 9.8±0.37 (445) ^b | 36±1.7 | 46±1.9 |
| | HL | 0.32±0.04 (118) ^b | 6±0.10 (114) ^b | 0.515±0.00 (76) ^c | 0.222±0.01 (44) ^b | 0.384±0.04 (86) ^b | 106±54 (93) ^a | 273±128 (110) ^a | 1.6±0.20 (73) ^a | 29±0.6 | 206±39 |

777

778 Table 2. Effect of atrazine ($50 \mu\text{g L}^{-1}$), ML & HL exposure and the combined effect (light and atrazine) on
 779 light energy conservation indicator (PI_{ABS}), non-photochemical quenching (qE_{max}), and ROS content, in
 780 percentage from control (control is taken as 100%). Data are means \pm SD of two independent experiments in
 781 triplicate. Within treatments, values followed by one asterisk are significantly different from the control, and
 782 values followed by two asterisks indicate significant differences between the LL and ML or HL exposure,
 783 while values followed by three asterisks are significantly different from both control and ML and HL treatment
 784 (Tukey's HSD, $P < 0.05$).

| Species | Parameter | Effect of atrazine % | | | | |
|---------|--------------------------|--|--|--|--|--|
| | | Effect of atrazine % of the control (\pm) LL | Effect of ML % of the control (\pm) | Atrazine+ ML % of the control (\pm) | Effect of HL % of the control (\pm) | Atrazine+ HL % of the control (\pm) |
| T-CN | PI_{ABS} | 2* (0) | 5** (0) | 29*** (2) | 5** (0) | 21*** (1) |
| A-CN | PI_{ABS} | 37* (2) | 75** (5) | 16*** (1) | 57** (1) | 11*** (1) |
| T-MB | PI_{ABS} | 52* (2) | 4** (0) | 5*** (0) | 3** (0) | 8*** (0) |
| A-MP | PI_{ABS} | 10* (1) | 48** (2) | 28*** (2) | 40** (2) | 15 (1) |
| T-CN | qE_{max} | 85* (9) | 28** (2) | 37*** (1) | 26** (2) | 24*** (2) |
| A-CN | qE_{max} | 78* (3) | 118 (16) | 40*** (2) | 124** (15) | 28*** (3) |
| T-MB | qE_{max} | 97 (5) | 73** (6) | 86 (5) | 66** (3) | 70*** (7) |
| A-MP | qE_{max} | 81* (3) | 183** (24) | 42*** (3) | 189** (19) | 23*** (2) |
| T-CN | ROS | 171* (12) | 101 (10) | 131*** (14) | 114 (10) | 138*** (21) |
| A-CN | ROS | 243* (18) | 163** (21) | 466*** (42) | 227** (32) | 286*** (25) |
| T-MB | ROS | 444* (72) | 107 (7) | 162*** (12) | 116 (17) | 231*** (18) |
| A-MP | ROS | 176* (12) | 105 (8) | 113*** (17) | 36** (4) | 390*** (47) |



786

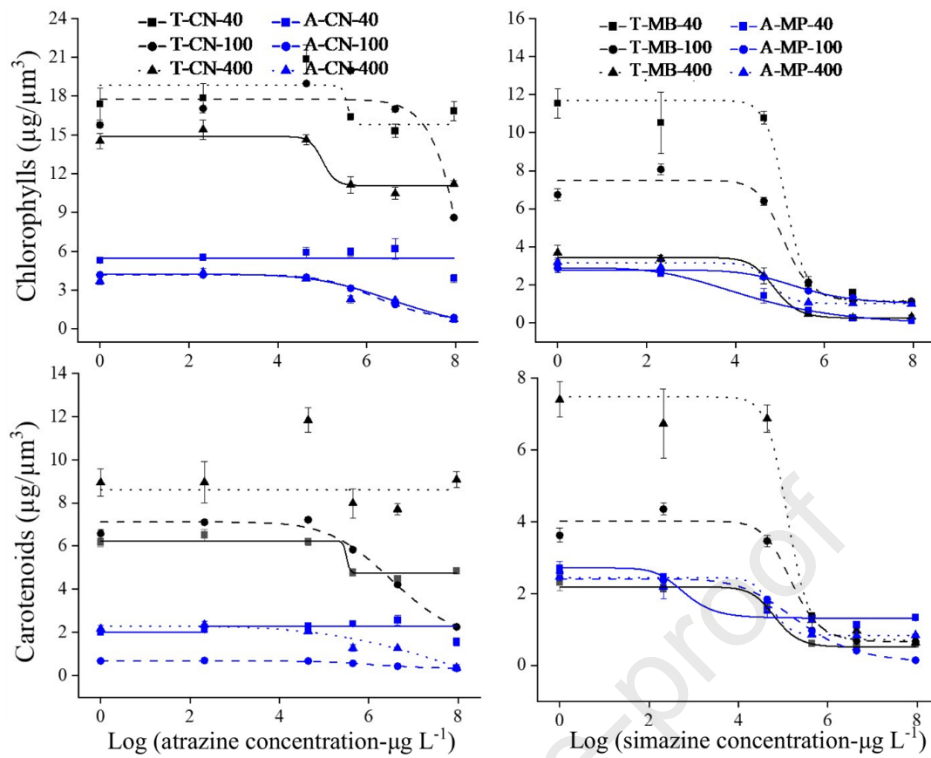
787

788

789

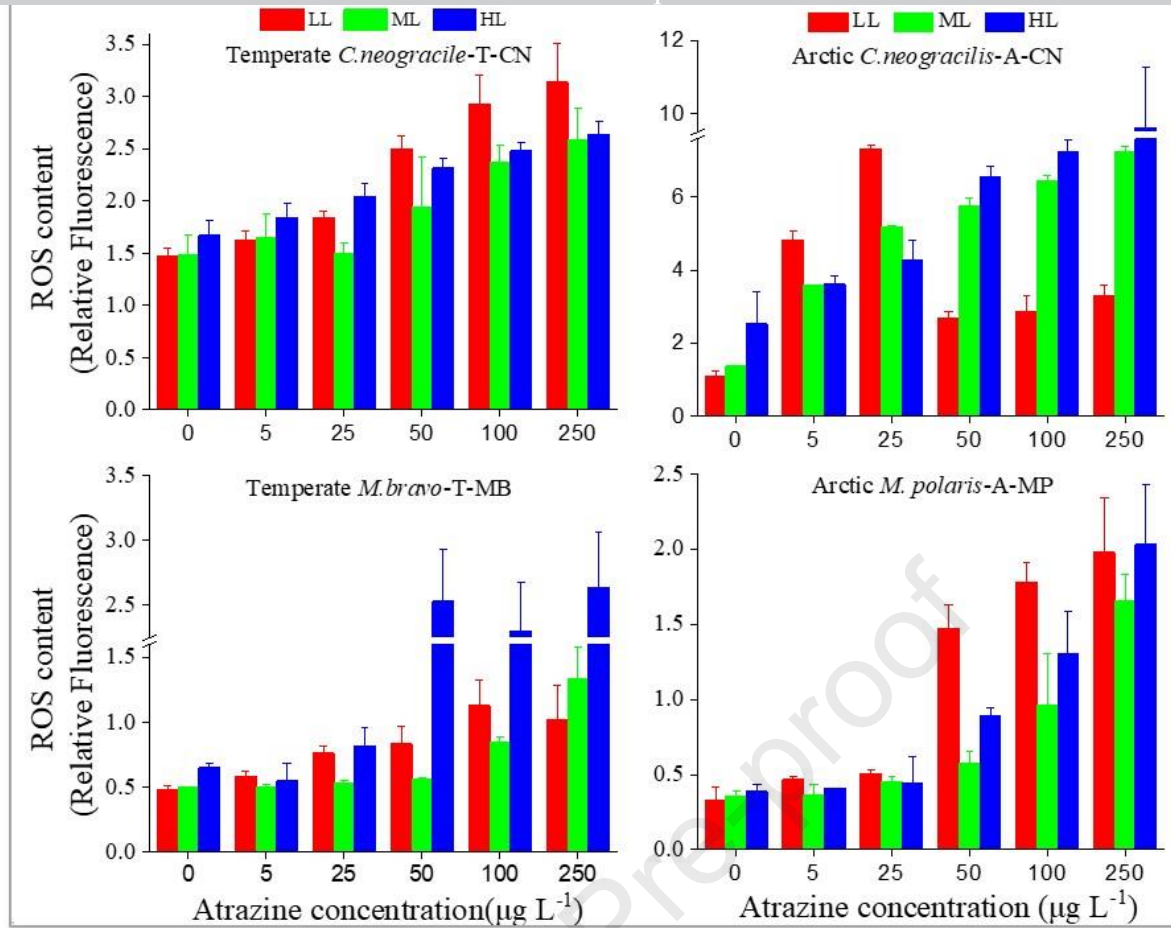
Figure 1. The effect of atrazine and simazine on the growth rate of four species (temperate *C. neogracile* (T-CN), Arctic *C. neogracilis* (A-CN), temperate *M. bravo* (T-MB), and Arctic *M. polaris* (A-MP)) after 72 h exposure under LL (square), ML (circle) and HL (triangle). Data expressed as means \pm SD (n = 6)

790



791

792 Figure 2. The effect of atrazine (after 72 h) on the pigment content of four microalgal species (temperate *C.*
 793 *neogracile* (T-CN), Arctic *C. neogracilis* (A-CN), temperate *M. bravo* (T-MB), and Arctic *M. polaris* (A-MP))
 794 under LL (square), ML (circle) and HL (triangle) light intensities. The presented data calculated is relative to
 795 cell biovolume (μm^3), data expressed as means \pm SD (n = 6).



796

797

798

799

Figure 3. The effect of atrazine on ROS content of the studied species (temperate *C. neogracile* (T-CN), Arctic *C. neogracilis* (A-CN), temperate *M. bravo* (T-MB), and Arctic *M. polaris* (A-MP)) after 72 h exposure under LL, ML and HL. Data expressed as means \pm SD (n = 6).

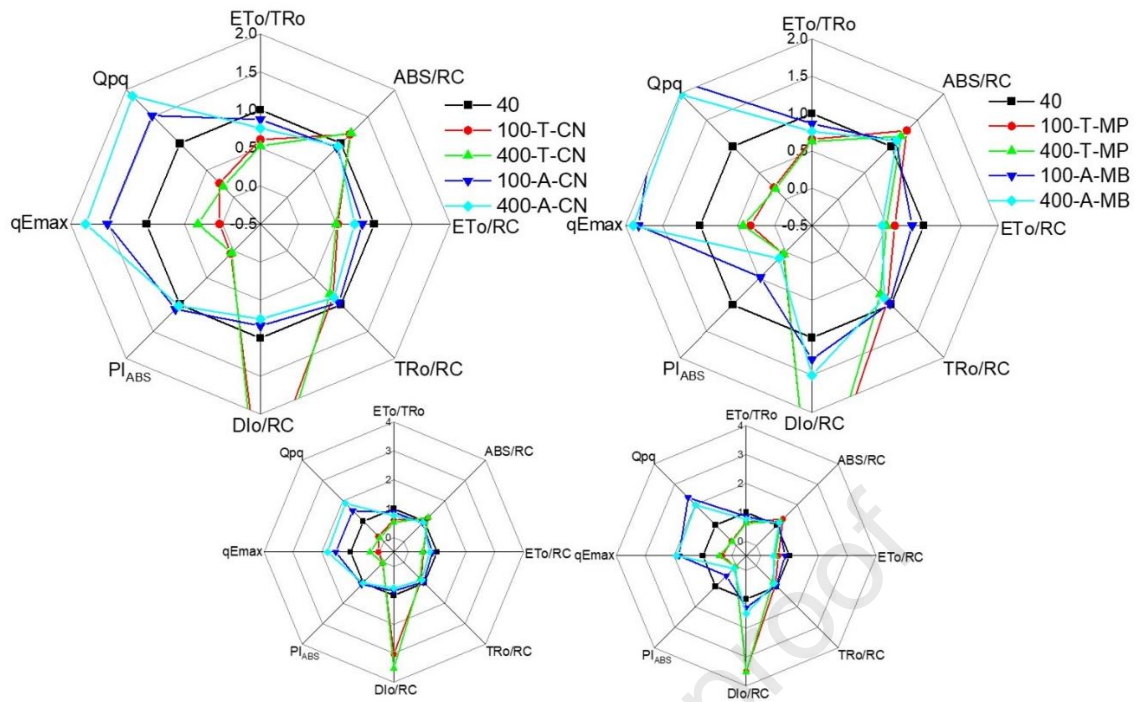
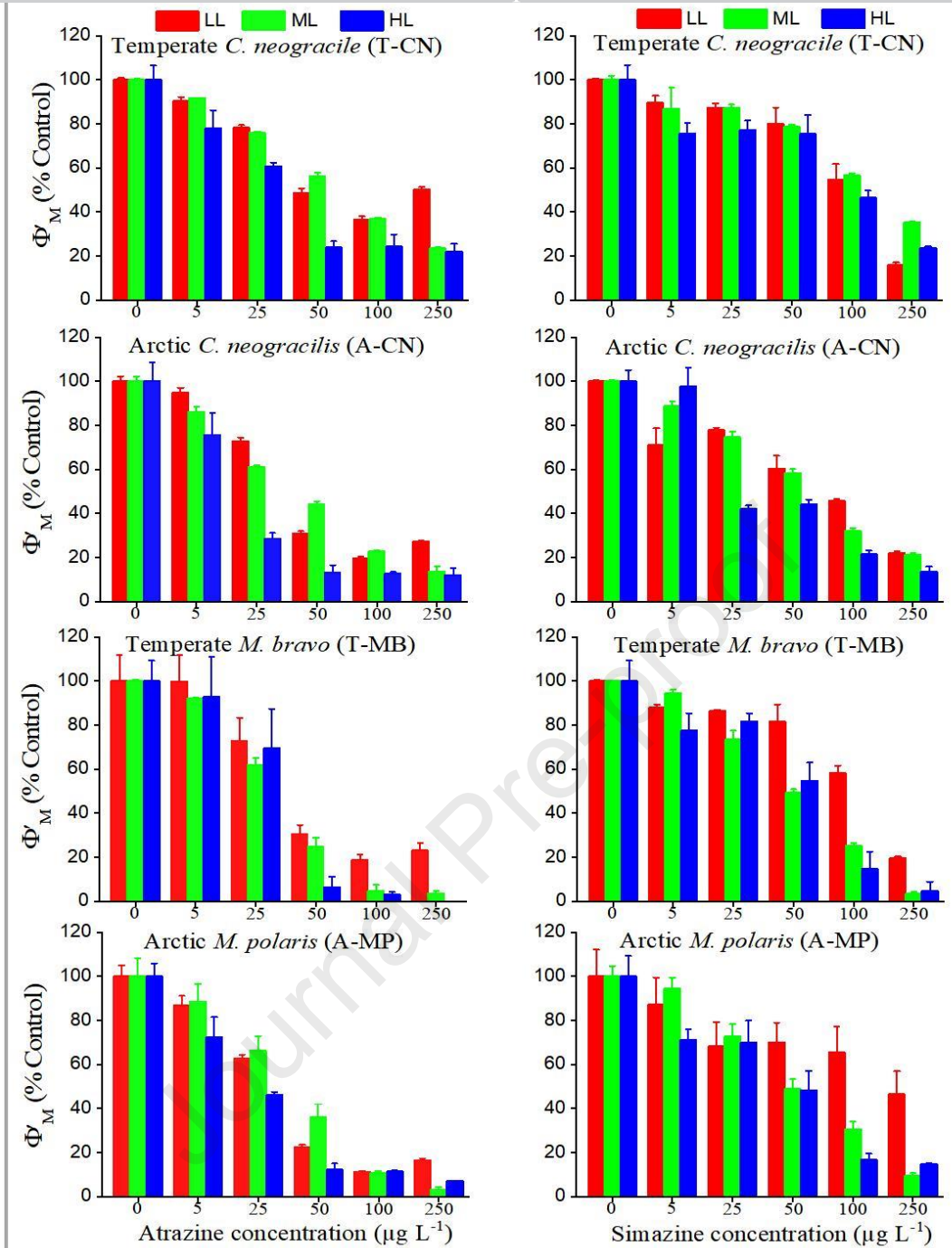


Figure 4. The effect of growth light intensity (LL, ML, and HL) on the PSII energy fluxes of temperate *C. neogracile* (T-CN), Arctic *C. neogracilis* (A-CN), temperate *M. bravo* (T-MB), and Arctic *M. polaris* (A-MP). Data expressed as means \pm SD (n = 6).

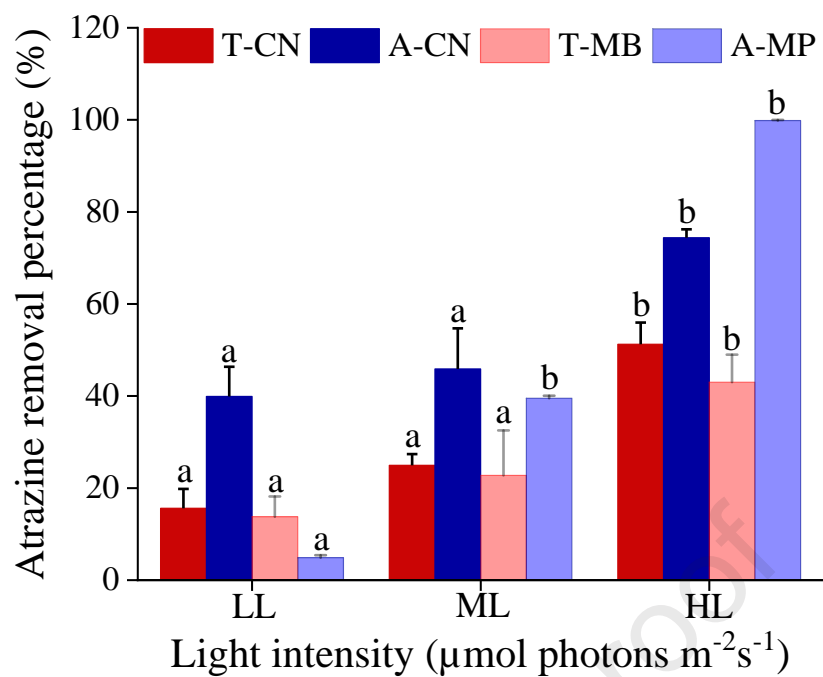


806

807 Figure 5. The effect of atrazine and simazine on the PSII operational quantum yield (Φ'_M) of temperate *C.*808 *neogracile* (T-CN), Arctic *C. neogracilis* (A-CN), temperate *M. bravo* (T-MB), and Arctic *M. polaris* (A-MP)809 after 72 h exposure under LL, ML and HL conditions. Data expressed as means \pm SD (n = 6).

810

811



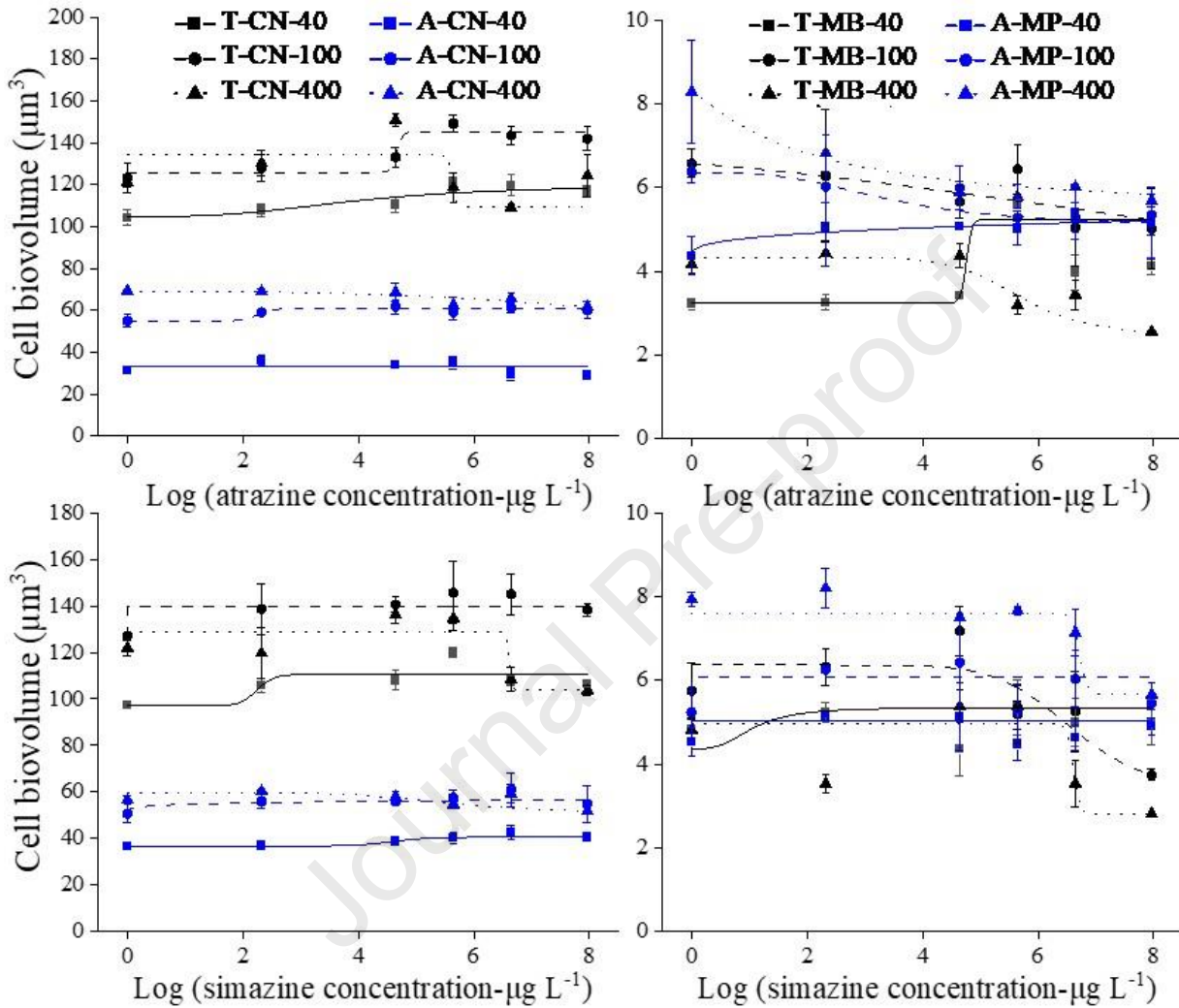
812

813 Figure 6. The concentration of atrazine removed from the growth medium for (red color) temperate *C.*
 814 *neogracile* (T-CN) and temperate *M. bravo* (T-MB), (blue color) Arctic *C. neogracilis* (A-CN) and Arctic *M.*
 815 *polaris* (A-MP) after 72 h exposure to $50 \mu\text{g L}^{-1}$ under LL, ML and HL conditions. Data expressed as means
 816 \pm SD (n = 6).

817

Supplementary Material

Figure S1. The effect of atrazine and simazine on the cell biovolume of the temperate *C. neogracile* (T-CN), Arctic *C. neogracilis* (A-CN), temperate *M. bravo* (T-MB), and Arctic *M. polaris* (A-MP) after 72 h exposure under LL, ML, and HL. Data expressed as means \pm SD (n = 6).



822

823

824 Table S1. In this study, parameters of fluorescence were defined.

| Parameters | Definition |
|---|--|
| Φ_M | Maximal PSII quantum yield |
| Φ'_M | Operational PSII quantum yield |
| NPQ | Non-photochemical quenching |
| NPQmax | Maximum ability for dissipation of excess energy |
| rETRmax | Maximum relative photosynthetic electron transport rate |
| α | Maximum light efficiency use |
| E_K | Light saturation coefficient |
| Specific energy fluxes (per Q_A reducing PSII RC) | |
| ABS/RC | Absorption flux (of antenna Chls) per RC (also a measure of PSII apparent antenna size) |
| TRo/RC | Trapped energy flux (leading to Q_A reduction) per RC |
| ETo/RC | Electron transport flux (further than Q_A^-) per RC |
| DIo/RC | Dissipated energy flux per RC |
| Performance index | |
| $PI_{ABS}=(RC/ABS)$ | Performance index (potential) for energy conservation from photons absorbed by PSII to the reduction of intersystem electron acceptors |

825

Highlights

- Photoadaptation processes are different between Arctic and temperate microalgae
- Arctic and temperate microalgae have different sensitivities to two herbicides
- High light enhances the impacts of herbicides on energy dissipation and photosynthesis of microalgae
- Atrazine removal by algae increased under high light
- These findings have applications for Arctic and temperate microalgae living in fluctuating light environments
-

Journal Pre-proof

JD, BEB, JL and PJ conceived and designed the experiments, gave technical support and conceptual advice. JD, DI, LO and LS performed the analysis. JD, HFX, BEB, JL and PJ wrote manuscript. DI, HFX, LO, LS provided technical and editorial assistance. All authors read and approved the manuscript.

Journal Pre-proof

Declaration of interests

The authors declare that they have no known competing financial interests or personal relationships that could have appeared to influence the work reported in this paper.

The authors declare the following financial interests/personal relationships which may be considered as potential competing interests:

Philippe Juneau reports financial support was provided by Natural Sciences and Engineering Research Council of Canada.

Journal Pre-proof